ASTRONOMY & ASTROPHYSICS
SUPPLEMENT SERIES

Astron. Astrophys. Suppl. Ser. **126,** 105-111 (1997)

Atomic data from the IRON Project

XXIV. Electron excitation of Li-like Fe XXIV between the $n = 2$ and $n' = 2$, 3, 4 fine-structure levels

K.A. Berrington[1] **and J.A. Tully**[2]

[1] Department of Applied Mathematics & Theoretical Physics, The Queen's University of Belfast, Belfast BT7 1NN, UK
[2] Département G.D. Cassini, Observatoire de la Côte d'Azur, BP. 4229, 06304 Nice Cedex 4, France

Received January 20; accepted March 3, 1997

Abstract. Collision strengths for electron induced transitions in Li-like Fe XXIV are calculated using a Breit-Pauli R-matrix technique. The target has 15 fine structure states corresponding to $n \leq 4$. Autoionizing resonances are found to affect 18 of the 39 collision strengths, namely those for transitions $2lj \rightarrow n'l'j'$ where $n' = 2, 3$. The present calculation is carried out only for electrons incident on the ground state with energies not exceeding 265 Ry. Beyond this we use the relativistic distorted wave collision strengths of Zhang et al. in order to complete our results. Thermally averaged collision strengths are computed and tabulated as functions of $\log T$ for transitions out of the $2s_{1/2}$, $2p_{1/2}$ and $2p_{3/2}$ states. The temperature range considered is $6.2 \leq \log T \leq 8.0$, Fe XXIV having its maximum coronal abundance when $\log T = 7.2$.

Key words: Li-like iron — electron collision — atomic data

1. Introduction

The present calculation is part of an international collaboration known as the IRON Project (Hummer et al. 1993, referred to as Paper I) to obtain accurate collision rates for fine-structure transitions. Other papers in the series are given in the References section, while a complete list of IRON Project published papers and those in press is available at http://www.am.qub.ac.uk.

Collisionally induced transitions in Fe XXIV have been examined by several authors in the past, most of whom used distorted wave (DW) approximations with some allowance for relativistic effects. To our knowledge, Hayes (1979) is the only person who has done a close-coupling (CC) calculation for this ion. Her method, however, did not take account of exchange and furthermore she only applied it to one energy above the excitation thresholds of her target in order to confirm that the coupling potentials could be neglected and that the DW approximation was sufficiently reliable. Hayes found that her CC and DW collision strengths at this particular energy agreed to within 5% for most transitions, except for $2p - 3s$ where the difference was about 20%.

The results given by Hayes (1979), Mann (1983), Younger (1987) and Zhang et al. (1990) are from DW calculations, which are similar in so far as they all take account of relativistic effects but ignore channel coupling and therefore show no resonance structure. For this reason we confine our comparison to the most recent work, namely that of Zhang et al. (1990).

2. The calculation

Paper I gives the basic atomic theory, approximations and computer codes employed in the IRON Project. The CC approximation known as the R-matrix method is used. In the present case we have taken account of channel coupling up to the $n = 4$ levels. Relativistic effects are allowed for as explained later.

The radial orbitals for the Li-like target are as follows: P_{1s}, P_{2s} are from Clementi & Roetti (1974). P_{2p} is the 2 exponent function

$$P_{2p}(r) = 584.527\, r^2 \exp(-12.0960\, r) + 35.5799\, r^2 \exp(-27.4414\, r), \quad (1)$$

which we obtained by using Hibbert's (1975) variational program CIV3 to minimise the energy of the $1s^2\,2p$ term. P_{3s} and P_{3d} are from Tully et al. (1990). Each remaining orbital P_{nl}, with $n\,l = 3p, 4s, 4p, 4d, 4f$, has the minimum number of exponents dictated by nl. The values of these exponents were calculated using CIV3 to minimise the appropriate $1s^2nl$ term energy. The orbital exponents for $n = 3, 4$ are given in Table 1.

Table 1. Exponents for the Fe^{+23} radial orbitals with analytic form similar to that in (1). The coefficients are fixed by orthonormality conditions

P_{nl}	r^1	r^2	r^3	r^4
3s	14.437	7.9574	8.0058	
3p		9.600263	7.847094	
3d			8.0050	
4s	13.360597	6.031843	6.055029	6.021776
4p		8.209951	5.974792	5.957608
4d			6.367924	5.971795
4f				6.000065

Although configuration interaction (CI) wavefunctions are used to describe the target terms, in practice each term is dominated by a single configuration. The target energies used in the collision calculation were, with one important exception, adjusted to match the accurate experimental levels of Reader et al. (1992). These are given in Table 2 after being converted to Ry (1 Ry = 109737.32 cm^{-1}). The exception concerns each pair of $4l$ fine-structure levels which we forced to be degenerate with the corresponding LS term.

Table 2. Fe XXIV: observed level energies E_i(obs) in Ry from Reader et al. (1992). $\Delta = E_i(\mathrm{BP}) - E_i(\mathrm{obs})$, where E_i(BP) is from the Breit-Pauli R-matrix calculation

i	Term	j	E_i(obs)	uncertainty	Δ
1	2s ^{2}S	1/2	0.0		
2	2p ^{2}P	1/2	3.57201	0.00007	0.004
3		3/2	4.74549	0.00013	−0.014
4	3s ^{2}S	1/2	84.497	0.015	0.034
5	3p ^{2}P	1/2	85.461	0.024	0.048
6		3/2	85.815	0.025	0.024
7	3d ^{2}D	3/2	86.197	0.015	0.034
8		5/2	86.321	0.022	0.019
9	4s ^{2}S	1/2	113.584	0.006	0.035
10	4p ^{2}P	1/2	113.990	0.015	0.030
11		3/2	114.136	0.015	0.018
12	4d ^{2}D	3/2	114.266	0.020	0.050
13		5/2	114.321	0.025	0.040
14	4f ^{2}F	5/2	114.342	0.015	0.028
15		7/2	114.379	0.022	0.014

Theoretical LS-coupling oscillator strengths calculated using the present wavefunctions and observed transition energies (see Table 2) are compared in Table 3 with those which Peach et al. (1988) obtained in the Opacity Project. Our length (L) and velocity (V) forms agree well and there is also fairly good overall agreement between our length oscillator strengths and those of Peach et al. (1988). This suggests that our choice of wavefunctions is satisfactory for computing reliable collision data.

Table 3. Oscillator strengths for Fe^{+23} calculated in the length (L) and velocity (V) gauge, compared with those from the Opacity Project (Peach et al. 1988)

Transition	L	V	OP
2s − 2p	0.0525	0.0606	0.052
2s − 3p	0.386	0.383	0.386
2s − 4p	0.0956	0.0944	0.0955
3s − 3p	0.0881	0.0947	0.0875
3s − 4p	0.425	0.421	0.424
4s − 4p	0.122	0.126	0.121
2p − 3s	0.0170	0.0174	0.017
2p − 4s	0.00365	0.00376	0.0037
3p − 4s	0.0399	0.0395	0.0395
2p − 3d	0.684	0.683	0.683
2p − 4d	0.122	0.122	0.157
3p − 3d	0.0149	0.0171	0.0151
3p − 4d	0.599	0.597	0.598
4p − 3d	0.0123	0.0124	0.0123
4p − 4d	0.0263	0.0274	0.0268
3d − 4f	1.016	1.016	
4d − 4f	0.00076	0.00078	

Collision strengths for fine structure transitions are obtained from two R-matrix calculations which we now describe.

BP is a 15-level fine-structure calculation using the Breit-Pauli Hamiltonian version of the R-matrix program (Berrington et al. 1995). This is the most accurate approach when the collision energy is comparable to the level splitting in the target. This method was used in the scattering energy range up to the highest threshold.

JAJOM is a 9-term LS-coupling calculation plus a transformation to intermediate coupling which we apply to the reactance matrix using the JAJOM program written by Saraph (1978). This was used from just above the highest threshold up to a scattering energy of 265 Ry. For allowed transitions we use a "top-up" procedure which consists in assuming that beyond $J = 80$ the partial collision strengths form a geometrical series. In this way we are able to complete the sum to infinity of partial waves analytically.

For the purpose of comparing our results numerically with those of Zhang et al. (1990) we choose an energy that lies above the highest target term included in our calculation, namely 4f. The comparison is shown in Table 4

where it can be seen that differences are less than 10% for all transitions out of $2s_{1/2}$. For transitions from the 2p levels the differences are greater with some of them as high as 14%.

Table 4. A comparison of R-matrix (BP) and distorted-wave (DW) collision strengths for excitation of Fe^{+23} at 132.25 Ry. The DW results are from Zhang et al. (1990)

Transition	BP	DW
$2s_{1/2} - 2p_{1/2}$	0.254	0.253
$-2p_{3/2}$	0.472	0.475
$-3s_{1/2}$	0.0137	0.0151
$-3p_{1/2}$	0.0053	0.0054
$-3p_{3/2}$	0.0101	0.0099
$-3d_{3/2}$	0.0118	0.0118
$-3d_{5/2}$	0.0176	0.0177
$-4s_{1/2}$	0.0025	0.0029
$-4p_{1/2}$	0.0011	0.0010
$-4p_{3/2}$	0.0022	0.0020
$-4d_{3/2}$	0.0021	0.0020
$-4d_{5/2}$	0.0031	0.0030
$-4f_{5/2}$	0.0012	0.0011
$-4f_{7/2}$	0.0016	0.0014
$2p_{1/2} - 2p_{3/2}$	0.0196	0.0191
$-3s_{1/2}$	0.0011	0.0010
$-3p_{1/2}$	0.0142	0.0155
$-3p_{3/2}$	0.0034	0.0034
$-3d_{3/2}$	0.0609	0.0613
$-3d_{5/2}$	0.0065	0.0056

The approximations in each method are comparable at higher energies and any differences here are presumably caused by different "topping" up procedures and possibly by the fact that Zhang et al. (1990) use orbitals obtained by solving the Dirac equation with a Dirac-Fock-Slater potential. We expect really important differences to occur only at lower energies where resonance structures such as those shown in Figs. 1-2 and 4-7 occur. Resonances can have a big effect on effective collision strengths, as seen in Figs. 8 and 9.

Thermal averaging of the collision strengths is done using the "linear interpolation" method described by Burgess & Tully (1992). The resulting effective collision strengths Υ are given in Table 5 for the astrophysically important temperature range $6.2 \leq \log T \leq 8.0$ where Fe^{+23} is abundant under conditions of coronal ionization equilibrium (see Arnaud & Rothenflug 1985). For temperatures below two million degrees the abundance will be negligible. For this reason we begin our tabulation of Υ in Table 5 at $\log T = 6.2$. Astrophysical situations may exist where Fe^{+23} is abundant at temperatures lower than this; in these cases one would need to extend the temperature range below $10^{6.2}$ K. This should pose no problem since our collision strengths will be preserved for posterity at the CDS (Centre de données astronomiques de Strasbourg) and some other databanks.

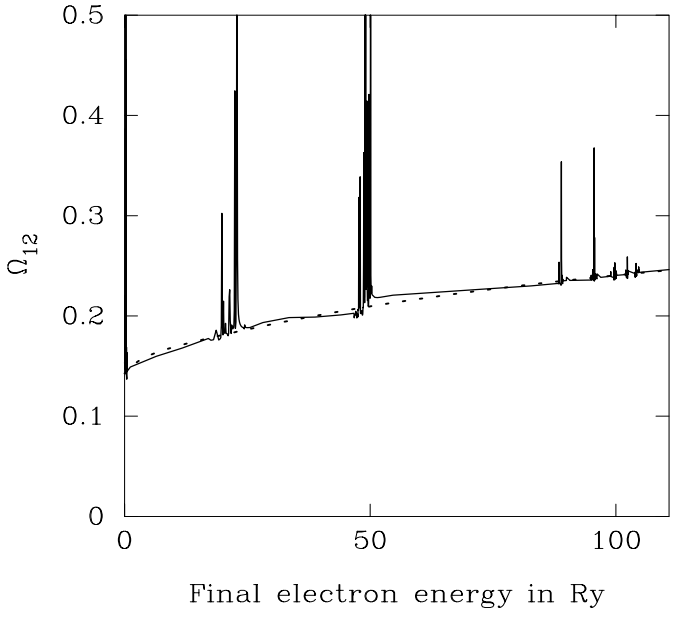

Fig. 1. $Fe^{+23}(2s_{1/2} \rightarrow 2p_{1/2})$ collision strength shown over the range $0 \leq E_f \leq 110.80699$ (i.e. from $2p_{1/2}$ to $4f_{7/2}$). Full line: present Breit-Pauli calculation; broken line: DW calculation by Zhang et al. (1990)

3. Discussion of resonances and their effect on Υ

Of our energy dependent collision strengths only those for the 18 transitions between $n = 2$ and $n' = 2, 3$ are perturbed by autoionising resonances. In some cases the resonances greatly increase the effective collision strengths. But in general this happens at temperatures below a million degrees so it is not of particular astrophysical significance since, as mentioned earlier, under conditions of coronal ionization equilibrium the abundance of Fe^{+23} is essentially zero at such "low" temperatures.

It would be tedious to discuss in detail the energy dependence of each of the 39 collision strengths we have calculated. Here we select a few cases which serve to illustrate the main features. For conciseness and convenience we label the target energy levels nl_j in ascending order with the index shown in Table 2. This starts at 1 for the ground level ($2s_{1/2}$) and ends at 15 for the highest level ($4f_{7/2}$).

Transitions $1 \rightarrow 2$ and $1 \rightarrow 3$ are optically allowed and, apart from their numerical values, the collision strengths Ω_{12} and Ω_{13} have almost identical resonance patterns. Figure 1 shows Ω_{12} from threshold up to the energy of the $4f_{7/2}$ level. Note that we plot Ω against the final electron energy E_f in Rydberg units. The initial energy of the colliding electron E_i relative to the the lower state is

Table 5. Fe^{+23} effective collision strengths for $6.2 \leq \log T \leq 8.0$

Transition	6.2	6.4	6.6	6.8	7.0	7.2	7.4	7.6	7.8	8.0
$2s_{1/2} - 2p_{1/2}$	1.661^{-1}	1.747^{-1}	1.853^{-1}	1.976^{-1}	2.117^{-1}	2.278^{-1}	2.459^{-1}	2.659^{-1}	2.873^{-1}	3.095^{-1}
$2s_{1/2} - 2p_{3/2}$	3.172^{-1}	3.331^{-1}	3.523^{-1}	3.744^{-1}	4.000^{-1}	4.298^{-1}	4.642^{-1}	5.027^{-1}	5.445^{-1}	5.884^{-1}
$2s_{1/2} - 3s_{1/2}$	1.603^{-2}	1.562^{-2}	1.522^{-2}	1.493^{-2}	1.484^{-2}	1.499^{-2}	1.534^{-2}	1.581^{-2}	1.631^{-2}	1.677^{-2}
$2s_{1/2} - 3p_{1/2}$	5.573^{-3}	5.533^{-3}	5.566^{-3}	5.792^{-3}	6.328^{-3}	7.284^{-3}	8.747^{-3}	1.077^{-2}	1.339^{-2}	1.658^{-2}
$2s_{1/2} - 3p_{3/2}$	1.038^{-2}	1.041^{-2}	1.052^{-2}	1.097^{-2}	1.198^{-2}	1.378^{-2}	1.650^{-2}	2.027^{-2}	2.511^{-2}	3.101^{-2}
$2s_{1/2} - 3d_{3/2}$	1.280^{-2}	1.274^{-2}	1.263^{-2}	1.262^{-2}	1.284^{-2}	1.333^{-2}	1.408^{-2}	1.503^{-2}	1.608^{-2}	1.714^{-2}
$2s_{1/2} - 3d_{5/2}$	1.960^{-2}	1.954^{-2}	1.930^{-2}	1.920^{-2}	1.943^{-2}	2.009^{-2}	2.118^{-2}	2.264^{-2}	2.444^{-2}	2.644^{-2}
$2s_{1/2} - 4s_{1/2}$	2.497^{-3}	2.507^{-3}	2.526^{-3}	2.559^{-3}	2.621^{-3}	2.719^{-3}	2.842^{-3}	2.976^{-3}	3.105^{-3}	3.224^{-3}
$2s_{1/2} - 4p_{1/2}$	1.100^{-3}	1.128^{-3}	1.174^{-3}	1.251^{-3}	1.374^{-3}	1.562^{-3}	1.834^{-3}	2.204^{-3}	2.681^{-3}	3.262^{-3}
$2s_{1/2} - 4p_{3/2}$	2.176^{-3}	2.231^{-3}	2.323^{-3}	2.472^{-3}	2.705^{-3}	3.056^{-3}	3.564^{-3}	4.267^{-3}	5.184^{-3}	6.315^{-3}
$2s_{1/2} - 4d_{3/2}$	2.095^{-3}	2.090^{-3}	2.086^{-3}	2.086^{-3}	2.098^{-3}	2.129^{-3}	2.188^{-3}	2.277^{-3}	2.397^{-3}	2.537^{-3}
$2s_{1/2} - 4d_{5/2}$	3.168^{-3}	3.160^{-3}	3.154^{-3}	3.158^{-3}	3.177^{-3}	3.224^{-3}	3.311^{-3}	3.438^{-3}	3.598^{-3}	3.776^{-3}
$2s_{1/2} - 4f_{5/2}$	1.233^{-3}	1.212^{-3}	1.189^{-3}	1.166^{-3}	1.146^{-3}	1.133^{-3}	1.130^{-3}	1.136^{-3}	1.148^{-3}	1.164^{-3}
$2s_{1/2} - 4f_{7/2}$	1.646^{-3}	1.618^{-3}	1.587^{-3}	1.556^{-3}	1.529^{-3}	1.511^{-3}	1.506^{-3}	1.515^{-3}	1.538^{-3}	1.568^{-3}
$2p_{1/2} - 2p_{3/2}$	3.734^{-2}	4.120^{-2}	4.291^{-2}	4.166^{-2}	3.807^{-2}	3.346^{-2}	2.896^{-2}	2.516^{-2}	2.225^{-2}	2.017^{-2}
$2p_{1/2} - 3s_{1/2}$	4.738^{-3}	3.722^{-3}	2.950^{-3}	2.383^{-3}	2.004^{-3}	1.796^{-3}	1.748^{-3}	1.846^{-3}	2.076^{-3}	2.420^{-3}
$2p_{1/2} - 3p_{1/2}$	1.650^{-2}	1.604^{-2}	1.562^{-2}	1.529^{-2}	1.513^{-2}	1.517^{-2}	1.538^{-2}	1.569^{-2}	1.602^{-2}	1.634^{-2}
$2p_{1/2} - 3p_{3/2}$	7.156^{-3}	6.702^{-3}	5.999^{-3}	5.245^{-3}	4.568^{-3}	4.024^{-3}	3.626^{-3}	3.363^{-3}	3.214^{-3}	3.154^{-3}
$2p_{1/2} - 3d_{3/2}$	5.389^{-2}	5.534^{-2}	5.734^{-2}	6.046^{-2}	6.524^{-2}	7.223^{-2}	8.188^{-2}	9.456^{-2}	1.104^{-1}	1.293^{-1}
$2p_{1/2} - 3d_{5/2}$	1.267^{-2}	1.189^{-2}	1.063^{-2}	9.202^{-3}	7.834^{-3}	6.629^{-3}	5.633^{-3}	4.859^{-3}	4.296^{-3}	3.913^{-3}
$2p_{1/2} - 4s_{1/2}$	4.298^{-4}	4.128^{-4}	3.933^{-4}	3.730^{-4}	3.549^{-4}	3.437^{-4}	3.448^{-4}	3.626^{-4}	3.989^{-4}	4.533^{-4}
$2p_{1/2} - 4p_{1/2}$	2.745^{-3}	2.734^{-3}	2.723^{-3}	2.721^{-3}	2.741^{-3}	2.794^{-3}	2.873^{-3}	2.958^{-3}	3.038^{-3}	3.104^{-3}
$2p_{1/2} - 4p_{3/2}$	1.402^{-3}	1.343^{-3}	1.268^{-3}	1.179^{-3}	1.081^{-3}	9.818^{-4}	8.916^{-4}	8.177^{-4}	7.634^{-4}	7.283^{-4}
$2p_{1/2} - 4d_{3/2}$	9.901^{-3}	1.011^{-2}	1.043^{-2}	1.091^{-2}	1.161^{-2}	1.261^{-2}	1.396^{-2}	1.573^{-2}	1.793^{-2}	2.054^{-2}
$2p_{1/2} - 4d_{5/2}$	2.571^{-3}	2.432^{-3}	2.253^{-3}	2.035^{-3}	1.790^{-3}	1.534^{-3}	1.290^{-3}	1.070^{-3}	8.847^{-4}	7.351^{-4}
$2p_{1/2} - 4f_{5/2}$	1.698^{-3}	1.711^{-3}	1.742^{-3}	1.802^{-3}	1.900^{-3}	2.046^{-3}	2.245^{-3}	2.492^{-3}	2.772^{-3}	3.063^{-3}
$2p_{1/2} - 4f_{7/2}$	1.051^{-3}	9.836^{-4}	8.993^{-4}	8.017^{-4}	6.971^{-4}	5.947^{-4}	5.035^{-4}	4.299^{-4}	3.760^{-4}	3.402^{-4}
$2p_{3/2} - 3s_{1/2}$	1.044^{-2}	8.312^{-3}	6.629^{-3}	5.355^{-3}	4.483^{-3}	3.996^{-3}	3.872^{-3}	4.084^{-3}	4.604^{-3}	5.392^{-3}
$2p_{3/2} - 3p_{1/2}$	8.007^{-3}	7.342^{-3}	6.490^{-3}	5.632^{-3}	4.886^{-3}	4.303^{-3}	3.888^{-3}	3.624^{-3}	3.487^{-3}	3.444^{-3}
$2p_{3/2} - 3p_{3/2}$	4.098^{-2}	4.002^{-2}	3.863^{-2}	3.726^{-2}	3.624^{-2}	3.568^{-2}	3.556^{-2}	3.577^{-2}	3.616^{-2}	3.664^{-2}
$2p_{3/2} - 3d_{3/2}$	2.691^{-2}	2.621^{-2}	2.503^{-2}	2.390^{-2}	2.319^{-2}	2.314^{-2}	2.389^{-2}	2.552^{-2}	2.803^{-2}	3.134^{-2}
$2p_{3/2} - 3d_{5/2}$	1.108^{-1}	1.129^{-1}	1.156^{-1}	1.202^{-1}	1.279^{-1}	1.399^{-1}	1.569^{-1}	1.795^{-1}	2.080^{-1}	2.419^{-1}
$2p_{3/2} - 4s_{1/2}$	8.680^{-4}	8.342^{-4}	7.957^{-4}	7.566^{-4}	7.232^{-4}	7.053^{-4}	7.139^{-4}	7.576^{-4}	8.400^{-4}	9.600^{-4}
$2p_{3/2} - 4p_{1/2}$	1.376^{-3}	1.319^{-3}	1.246^{-3}	1.161^{-3}	1.068^{-3}	9.774^{-4}	8.972^{-4}	8.360^{-4}	7.998^{-4}	7.902^{-4}
$2p_{3/2} - 4p_{3/2}$	7.294^{-3}	7.216^{-3}	7.123^{-3}	7.040^{-3}	7.016^{-3}	7.078^{-3}	7.204^{-3}	7.349^{-3}	7.479^{-3}	7.580^{-3}
$2p_{3/2} - 4d_{3/2}$	5.102^{-3}	4.974^{-3}	4.820^{-3}	4.653^{-3}	4.499^{-3}	4.397^{-3}	4.387^{-3}	4.503^{-3}	4.759^{-3}	5.152^{-3}
$2p_{3/2} - 4d_{5/2}$	2.029^{-2}	2.056^{-2}	2.099^{-2}	2.169^{-2}	2.278^{-2}	2.440^{-2}	2.671^{-2}	2.981^{-2}	3.374^{-2}	3.846^{-2}
$2p_{3/2} - 4f_{5/2}$	1.908^{-3}	1.823^{-3}	1.721^{-3}	1.610^{-3}	1.502^{-3}	1.411^{-3}	1.350^{-3}	1.326^{-3}	1.338^{-3}	1.376^{-3}
$2p_{3/2} - 4f_{7/2}$	3.834^{-3}	3.812^{-3}	3.809^{-3}	3.850^{-3}	3.954^{-3}	4.142^{-3}	4.432^{-3}	4.821^{-3}	5.285^{-3}	5.787^{-3}

given by $E_i = E_f + E_{if}$, where E_{if} is the transition energy and can be obtained from Table 2. At $E_f \simeq 0$ there is an indication in Fig. 1 of some structure in the collision strength. Suspecting that this is caused by resonances converging on the level $2p_{3/2}$, we give a blow-up in Fig. 2 of the $2p_{1/2} - 2p_{3/2}$ energy interval ($0 \leq E_f \leq 1.17348$). Here we clearly see a number of narrow, well separated resonances. A striking amount of detail, which is completely hidden in Fig. 1, is now revealed. The apparently random way the peaks of these small resonances vary is caused by not using a sufficiently small steplength in energy for the purpose of scanning. To do so would greatly increase the amount of computing time required and make the whole calculation extremely arduous. The reason why resonances occur over less than half the interval is because the search for them was stopped after a finite number had been located. Figure 3 shows Υ_{12} as a function of temperature over the interval $4 \leq \log T \leq 8$. One can see a slight

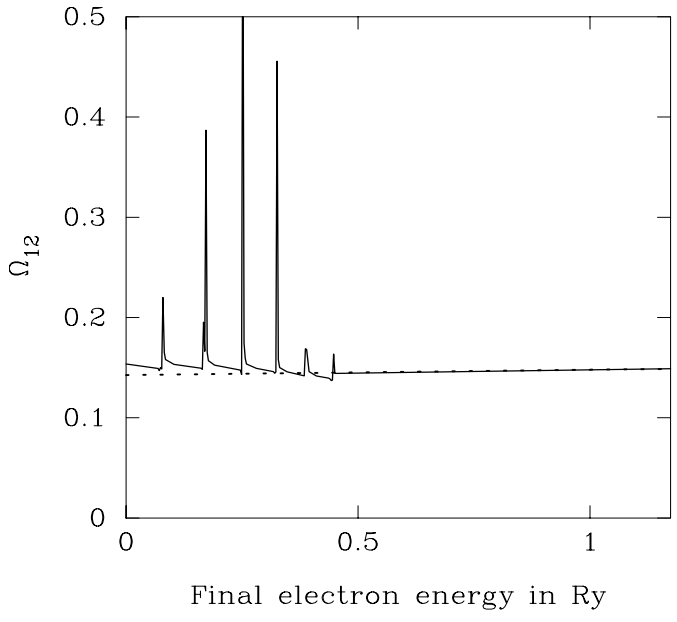

Fig. 2. $Fe^{+23}(2s_{1/2} \rightarrow 2p_{1/2})$ collision strength shown over the range $0 \leq E_f \leq 1.17348$ (i.e. from $2p_{1/2}$ to $2p_{3/2}$). Full line: present Breit-Pauli calculation; broken line: DW calculation by Zhang et al. (1990)

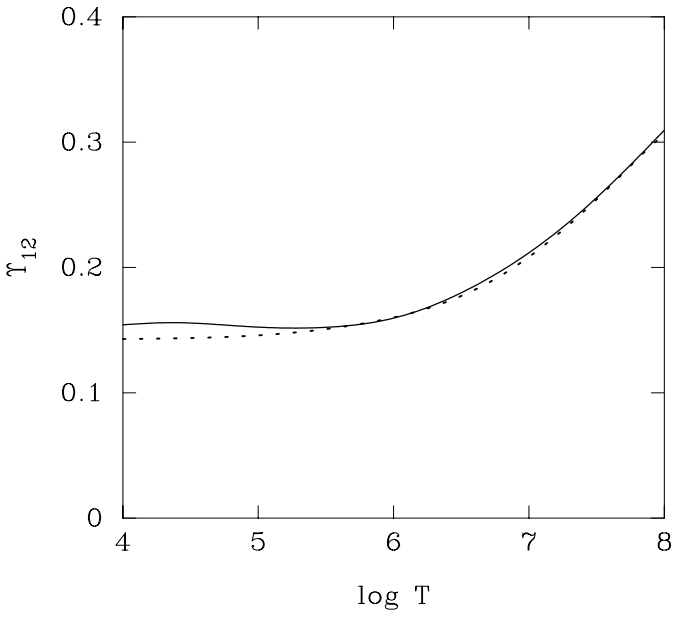

Fig. 3. $Fe^{+23}(2s_{1/2} \rightarrow 2p_{1/2})$ effective collision strength for the temperature range $4 \leq \log T \leq 8$. Full line: IRON Project; broken line: Zhang et al. (1990)

increase in Υ for temperatures below about 10^6. This is due to the resonances shown in Fig. 2; those at higher energies have a much smaller effect on Υ and produce a barely perceptible increase at temperatures above 10^6.

The optically forbidden transition $1 \rightarrow 4$ is a much more interesting case. Here we cover the range from $E_f = 0$ to the $4f_{7/2}$ level by means of four separate plots in order to illustrate the varied structure of the resonances. Figure 4 covers the range $0 \leq E_f \leq 0.96383$, which corresponds to the interval $3s_{1/2} - 3p_{1/2}$. A thick forest of resonances is seen to occur here. A comparable forest also occurs in Fig. 5 for the range $0.96383 \leq E_f \leq 1.31783$ (interval $3p_{1/2} - 3p_{3/2}$), while in Fig. 6 for the range $1.31783 \leq E_f \leq 1.69983$ (interval $3p_{3/2} - 3d_{3/2}$), the forest of resonances is preceded by a collection of isolated peaks. Between the levels $3d_{3/2}$ and $3d_{5/2}$ there are no resonances and no graph is shown. In Fig. 7, which covers the interval $3d_{5/2} - 4s_{1/2}$ ($1.82383 \leq E_f \leq 29.08683$), a striking series of Rydberg resonances appears. The process of delineation was stopped a short way from the $4s_{1/2}$ level after 5 groups of resonances had been delineated. Figure 8 shows that after thermal averaging the effect on Υ_{14} of all those resonances is considerable at temperatures below about one million degrees.

Finally, the transition $2 \rightarrow 3$, namely $2p_{1/2} - 2p_{3/2}$, is the only case encountered where resonances have a really big effect (50% increase above the background) at temperatures near ten million degrees, see Fig. 9.

The dotted curves shown in all graphs of Ω or Υ represent the DW calculations by Zhang et al. (1990). In order to make use of their tabulated collision strengths we first fitted them by cubic splines using the program OMEUPS (Burgess & Tully 1992). Each spline fit was then used to generate a tableau of collision strength values for the purpose of plotting. The same tableau was used to compute a thermally averaged collision strength in order to make a graphical comparison with the present IRON Project results.

Acknowledgements. This work was done with the support of a PPARC grant GR/K97608, and an EC network contract ERB CHRX CT920013. We thank David G. Hummer and Hong Lin Zhang for their constructive comments on an earlier version of the paper. The figures were prepared using the "trace vite et bien" graphics software written by Georges Gonczi at the Observatoire de la Côte d'Azur and available from http://www.obs-nice.fr/tvb/tvb.html.

References

Arnaud M., Rothenflug R., 1985, A&AS 60, 425
Bautista M.A., 1996, A&AS 119, 105 (Paper XVI)
Bautista M.A., 1997, A&AS 122, 167 (Paper XX)
Bautista M.A., Pradhan A.K., 1996, A&AS 115, 551 (Paper XIII)
Berrington K.A., 1995, A&AS 109, 193 (Paper VIII)
Berrington K.A., Pelan J.C., 1995, A&AS 114, 367 (Paper XII)
Berrington K.A., Eissner W.B., Norrington P.H., 1995, Comput. Phys. Commun. 92, 290
Burgess A., Tully J.A., 1992, A&A 254, 436
Butler K., Zeippen C.J., 1994, A&AS 108, 1 (Paper V)
Clementi E., Roetti C., 1974, Atom. Data Nucl. Data Tab. 14, 177

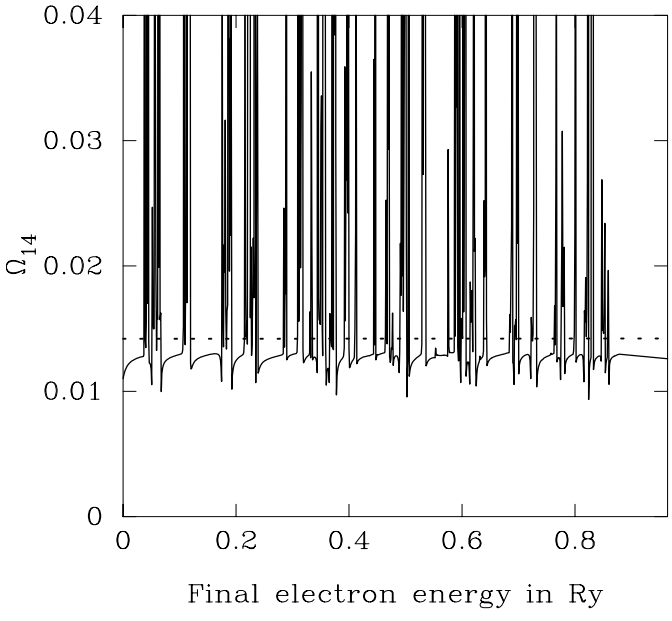

Fig. 4. $Fe^{+23}(2s_{1/2} \rightarrow 3s_{1/2})$ collision strength shown over the range $0 \leq E_f \leq 0.96383$ (i.e. from $3s_{1/2}$ to $3p_{3/2}$). Full line: present Breit-Pauli calculation; broken line: DW calculation by Zhang et al. (1990)

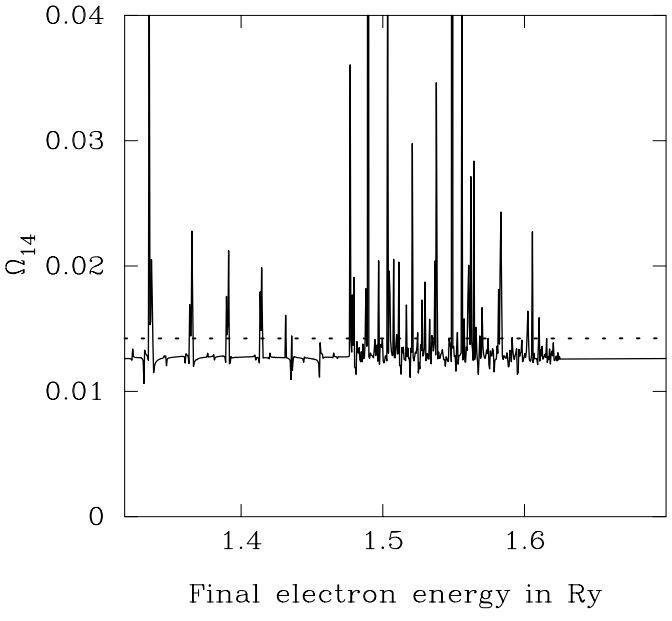

Fig. 6. $Fe^{+23}(2s_{1/2} \rightarrow 3s_{1/2})$ collision strength shown over the range $1.31783 \leq E_f \leq 1.69983$ (i.e. from $3p_{3/2}$ to $3d_{3/2}$). Full line: present Breit-Pauli calculation; broken line: DW calculation by Zhang et al. (1990)

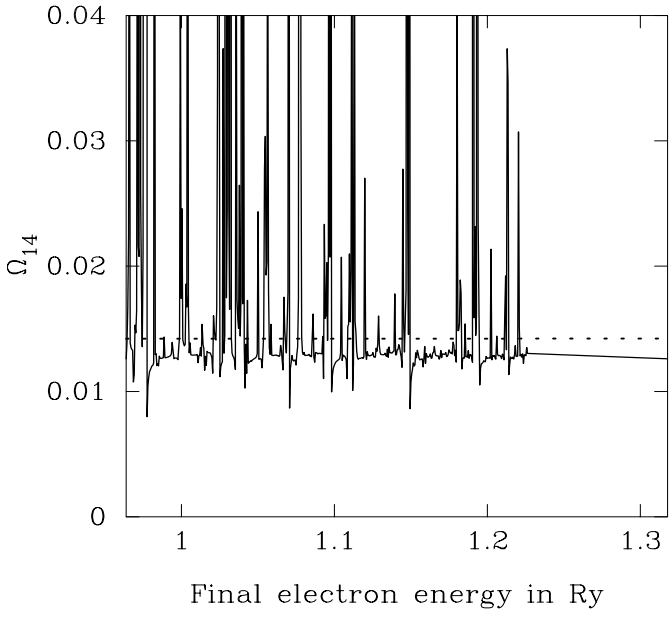

Fig. 5. $Fe^{+23}(2s_{1/2} \rightarrow 3s_{1/2})$ collision strength shown over the range $0.96383 \leq E_f \leq 1.31783$ (i.e. from $3p_{1/2}$ to $3p_{3/2}$). Full line: present Breit-Pauli calculation; broken line: DW calculation by Zhang et al. (1990)

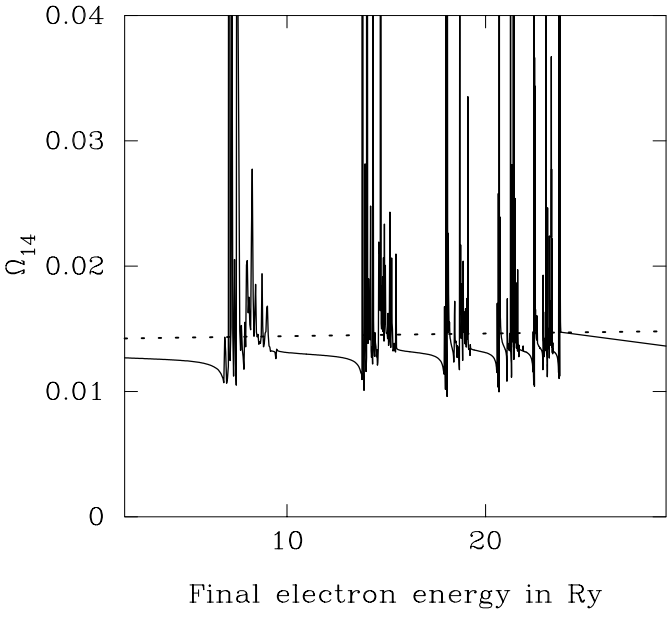

Fig. 7. $Fe^{+23}(2s_{1/2} \rightarrow 3s_{1/2})$ collision strength shown over the range $1.82383 \leq E_f \leq 29.08683$ (i.e. from $3d_{5/2}$ to $4s_{1/2}$). Full line: present Breit-Pauli calculation; broken line: DW calculation by Zhang et al. (1990)

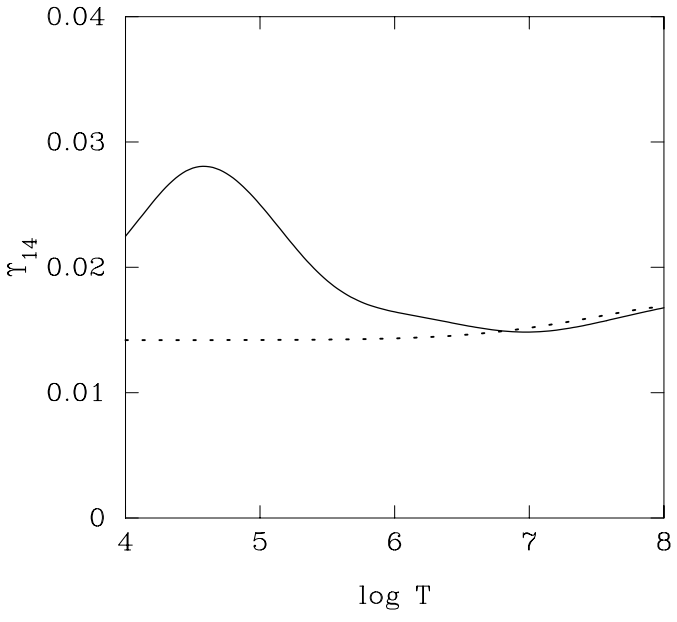

Fig. 8. $Fe^{+23}(2s_{1/2} \rightarrow 3s_{1/2})$ effective collision strength for the temperature range $4 \leq \log T \leq 8$. Full line: IRON Project; broken line: Zhang et al. (1990)

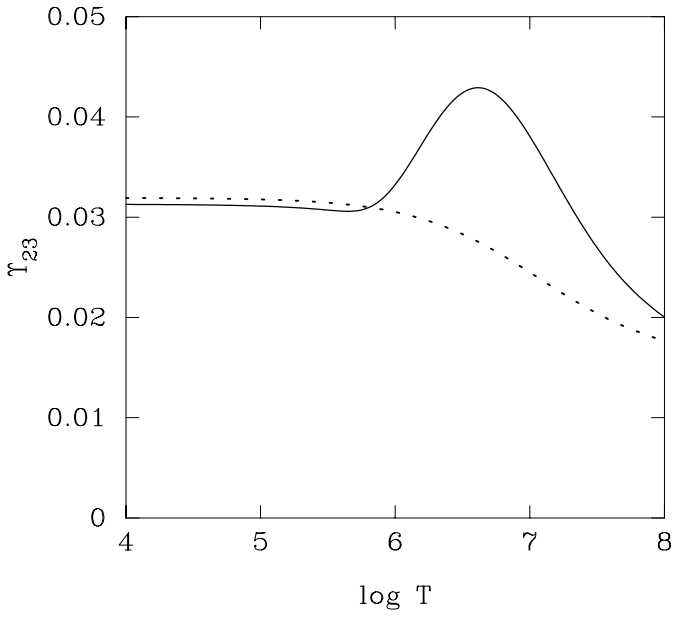

Fig. 9. $Fe^{+23}(2p_{1/2} \rightarrow 2p_{3/2})$ effective collision strength for the temperature range $4 \leq \log T \leq 8$. Full line: IRON Project; broken line: Zhang et al. (1990)

Galavís M.E., Mendoza C., Zeippen C.J., 1995, A&AS 111, 347 (Paper X)
Galavís M.E., Mendoza C., Zeippen C.J., 1997, A&AS 123, 159 (Paper XXII)
Hayes M.A., 1979, MNRAS 189, 55P
Hibbert A., 1975, Comput. Phys. Commun. 9, 141
Hummer D.G., Berrington K.A., Eissner W., Pradhan A.K., Saraph H.E., Tully J.A., 1993, A&A 279, 298 (Paper I)
Kisielius R., Berrington K.A., Norrington P.H., 1996, A&AS 118, 157 (Paper XV)
Lennon D.J., Burke V.M., 1994, A&AS 103, 273 (Paper II)
Mann J.B., 1983, Atom. Data Nucl. Data Tab. 29, 407
Nahar S.N., 1995, A&A 293, 967 (Paper VII)
Nahar S.N., Pradhan A.K., 1996, A&AS 119, 507 (Paper XVII)
Peach G., Saraph H.E., Seaton M.J., 1988, J. Phys. B: At. Mol. Opt. Phys. 21, 3669
Pelan J.C., Berrington K.A., 1995, A&AS 110, 209 (Paper IX)
Pelan J.C., Berrington K.A., 1997, A&AS 122, 177 (Paper XXI)
Quinet P., Le Dourneuf M., Zeippen C.J., 1996, A&AS 120, 361 (Paper XIX)
Reader J., Sugar J., Acquista N., Bahr R., 1992, J. Opt. Soc. Am. B 11, 1930
Saraph H.E., 1978, Comp. Phys. Commun. 15, 247
Saraph H.E., Tully J.A., 1994, A&AS 107, 29 (Paper IV)
Saraph H.E., Storey P.J., 1995, A&AS 115, 151 (Paper XI)
Storey P.J., Mason H.E., Saraph H.E., 1996, A&A 309, 677 (Paper XIV)
Tully J.A., Seaton M.J., Berrington K.A., 1990, J. Phys. B: At. Mol. Opt. Phys. 23, 3811
Younger S.M., 1987, Phys. Rev. A 36, 5432
Zhang H.L., Sampson D.H., Fontes C.J., 1990, Atom. Data Nucl. Data Tab. 44, 31
Zhang H.L., Graziani M., Pradhan A.K., 1994, A&A 283, 319 (Paper III)
Zhang H.L., Pradhan A.K., 1995, A&A 293, 953 (Paper VI)
Zhang H.L., 1996, A&AS 119, 523 (Paper XVIII)
Zhang H.L., Pradhan A.K., 1997, A&AS 123, 575 (Paper XXIII)